Pergamon

Bioorganic & Medicinal Chemistry 7 (1999) 763–772

BIOORGANIC & MEDICINAL CHEMISTRY

The Reactivity of Well Defined Diiron(III) Peroxo Complexes Toward Substrates: Addition to Electrophiles and Hydrocarbon Oxidation

Daniel D. LeCloux, Amy M. Barrios and Stephen J. Lippard*

Department of Chemistry, Massachusetts Institute of Technology, Cambridge, MA 02139, USA

Received 17 September 1998; accepted 6 October 1998

Abstract—The reactivity of previously reported peroxo adducts [Fe(μ-O_2)(μ-L)(O_2CPhCy)$_2$(1-Bu-Im)$_2$] (**1**), and [Fe(μ-O_2)(μ-L)(O_2CPhCy)$_2$(py)$_2$] (**2**), where L is a dinucleating ligand based on the *m*-xylylenediamine bis(Kemp's triacid imide), toward a variety of substrates is described. These studies were performed to probe the electronic properties of **1** and **2** and evaluate their potential as selective hydrocarbon oxidants. Compound **1** is nucleophilic at −77 °C, reacting with phenols and carboxylic acids to liberate hydrogen peroxide, whereas the less electron-rich pyridine analogue **2** is unreactive toward both reagents. By contrast, neither reacts at −77 °C with electrophilic reagents such as olefins or triphenylphosphine, or with weak hydrogen atom donors such as dimethylbenzylamine. When solutions of **1** are warmed to room temperature in solvents such as THF, toluene, and cyclopentane, mixtures of alcohol and ketone products derived from the solvent are formed. A detailed investigation of cyclopentane oxidation strongly points to a radical autoxidation pathway. These results are discussed in the context of the selective hydroxylation chemistry that occurs at the carboxylate-bridged diiron centers in soluble methane monooxygenase.

Introduction

The selective and efficient catalytic oxidation of hydrocarbon substrates under mild conditions continues to be a challenging goal for the synthetic chemist.[1–8] In Nature, obligate methanotrophic bacteria carry out one of the most difficult reactions of this kind, the conversion of methane to methanol under ambient conditions (eq (1)), by utilizing a soluble[9–11] or particulate[12,13] methane monooxygenase (sMMO or pMMO).

$$CH_4 + O_2 + NADH + H^+ \longrightarrow CH_3OH + H_2O + NAD^+ \quad (1)$$

The soluble form houses a carboxylate-bridged diiron center in its hydroxylase component (sMMOH), the site of methane oxidation. This protein is a member of a class of non-heme diiron enzymes which carry out a variety of selective hydrocarbon oxidative processes.[9,11] A closely related enzyme is ribonucleotide reductase, which reacts with O_2 at a diiron(II) center in its R2 subunit (RNR-R2) to generate a tyrosyl radical which in turn assists in the catalytic reduction of ribonucleotides. We seek to prepare functional synthetic models of these systems, with the dual goals of aiding in the elucidation of the biological O_2-activation mechanisms and of developing practical hydrocarbon oxidation catalysts.

The current state of knowledge regarding these systems, including structural, spectroscopic, and mechanistic information, is described in detail elsewhere;[9,14–16] therefore, only a brief synopsis is provided here. Oxygenated intermediates have been characterized for sMMO[10,17,18] and RNR-R2[19–23] by combining stopped-flow and rapid freeze quench methodologies with a variety of spectroscopic techniques. Both sMMOH and RNR-R2 react with O_2 in their diiron(II) forms to afford a diiron(III) peroxo species as the first detected intermediate. For sMMO, this unit converts to a diiron(IV) species, designated intermediate Q. It is intermediate Q or a closely related derivative which reacts with alkane substrates. Studies with radical clock[24] and chiral alkane[25] probes have provided compelling evidence against a hydrocarbon oxidation mechanism involving discrete substrate radicals. In RNR-R2, the peroxo intermediate converts to an oxo-bridged diiron(III)(IV) unit, X, possibly through a diiron(IV) intermediate like sMMO-Q. Intermediate X abstracts a hydrogen atom from a nearby tyrosine to yield a catalytically viable tyrosyl radical.

Much effort has been expended to mimic the oxidation chemistry of these non-heme iron enzymes. Iron(III)

Key words: Biomimetic reactions; oxygen; oxygenation.
*Corresponding author. Tel.: +1-1617-253-1892; fax: +1-617-258-8150.

0968-0896/99/$ - see front matter
PII: S0968-0896(98)00270-3

complexes have been treated with either hydrogen peroxide[26–30] or *tert*-butyl hydroperoxide[31–33] to generate an active oxidant. Modest selectivities for alcohol[27,31] or ketone[27,28] product have been observed in some cases. Careful examination has shown, however, that most of these oxidative systems operate through non-biomimetic, autoxidation pathways involving freely diffusing alkyl radicals.[30,33–39] One exception may be a stereospecific and presumably non-radical catalytic system composed of an Fe(II) tris(2-pyridylmethyl)amine complex and H_2O_2.[26]

By contrast, the reactivity of discrete, well defined diiron(III) peroxo complexes derived from iron(II) precursors and O_2 is essentially unexplored. Given that sMMO utilizes a reductive O_2 activation pathway, it is desirable to track an oxidation reaction in a model system from the dioxygen binding step, to formation of a high valent oxidant, and finally through the substrate oxidation event. Such a study would provide invaluable information for comparison with the enzyme and may spawn the development of practical hydrocarbon oxidation catalysts. Moreover, this approach may shed light on the composition, structure, and reactivity of intermediates postulated for synthetic iron oxidation systems. In the present article we provide a complete analysis of the reactivity of diiron(III) peroxo complexes derived from the *m*-xylylenediamine bis(Kemp's triacid)imide (H_2XDK) ligand system.[40]

Experimental

General considerations

The complexes [Fe_2(μ-O_2)(μ-PXDK)(μ-O_2CPhCy)(O_2-CPhCy)(Bu-Im)$_2$] (**1**) and [Fe_2(μ-O_2)(μ-BXDK)(μ-O_2-CPhCy)(O_2CPhCy)(py)$_2$] (**2**) were prepared from O_2 and the appropriate diiron(II) precursors at −77 °C according to an established procedure.[40] Authentic samples of 3,3′,5,5′-tetra-*tert*-butyl-1,1′-bi-2,2′-phenol,[41] cyclopentyl-hydroperoxide,[42] and 2-hydroxytetrahydrofuran,[43] were synthesized according to the literature methods, and their purity was confirmed by ^{1}H NMR and/or GC and GC/MS analyses. The presence of hydrogen peroxide was detected by using EM Quant® peroxide test strips, catalog number 10011-1, which were purchased from EM Science. Dioxygen (99.994%, Boc gases) was dried by passing the gas stream through a column of Drierite. Labeled dioxygen (95% $^{18}O_2$), toluene, and THF were purchased from Cambridge Isotope Laboratories, Inc. The solvents were vacuum transferred from Na/benzophenone ketyl. All other reagents were procured from commercial sources and used as received unless otherwise noted. THF, cyclopentane, toluene, pentane, and Et_2O were distilled from sodium benzophenone ketyl under nitrogen. Cyclopentane, isopentane, 1-hexene, and cyclohexene were distilled from sodium under nitrogen. Dichloromethane, 1,2-dichloroethane, and pyridine were distilled from CaH_2 under nitrogen. All air sensitive manipulations were carried out either in a nitrogen filled Vacuum Atmospheres drybox or by standard Schlenk line techniques at room temperature unless otherwise noted.

Physical measurements

NMR spectra were recorded on a Bruker AC-250 or Varian XL-300 spectrometer. FTIR spectra were recorded on a BioRad FTS-135 FTIR spectrometer.

GC and GC/MS

Analyses were carried out on a HP-5970 gas chromatograph connected to a HP-5971 mass analyzer. Alltech Econo-cap EC-WAX capillary columns of dimensions (15 m×0.53 mm×1.2 μm) and (30 m×0.25 mm×0.25 μm) were used for GC and GC/MS studies, respectively, except for triphenylphosphine and triphenylphosphine oxide, which were assayed with a HP-101 (12 m×0.2 mm ×0.2 mm) capillary column. The following method was used to effect nearly all separations: initial temperature = 50 °C; initial time = 10 min; temperature ramp = 50−200 °C at 10 deg/min. The products were identified by comparing their retention times and mass spectral patterns to those of authentic standards. Integrations were acquired by FID detection run in parallel to mass spectrometry by using an HP-3393 integrator. FID response calibration constants were measured by running calibration curves with authentic samples and an internal standard, either cyclopentanone or cyclohexanone.

For kinetic isotope or $^{18}O_2$ labeling studies, the ratio of isotopomers was determined by mass spectral integration of each parent ion. The integration response was assumed to be identical for the isotopomers.

Low-temperature UV–vis spectroscopy

Spectra were recorded on a HP8452A diode array spectrophotometer by using a custom manufactured immersion dewar, equipped with a 3 mL cell (1-cm pathlength) with quartz windows connected to a 14/20 female joint via a 10-cm long glass tube. A temperature of −77 °C was maintained with a dry ice/acetone bath and monitored with a Sensortek Model BAT-12 thermocouple thermometer.

Resonance Raman spectroscopy

Raman data were acquired by using a Coherent Innova 90 Kr^+ laser with an excitation wavelength of 647.1 nm and 65 mW of power. A 0.6-m single monochromator (1200 grooves/mm grating), with an entrance slit of 100 μm, and a liquid nitrogen cooled-CCD detector (Princeton Instruments, Inc.) were used in a standard backscattering configuration. A holographic notch filter (Kaiser Optical Systems) was used to attenuate Rayleigh scattering. Spectra of all samples were collected in toluene solution at −77 °C with the same custom-manufactured dewar used to acquire low-temperature UV–vis spectra. Solute concentrations were made as high as possible depending on the solubility of the reduced sample, ~20 mM in the best cases, to ensure an optimal signal-to-noise ratio. High vacuum line techniques were

used to transfer $^{18}O_2$ and to manipulate the resulting samples. A total of 1000 scans each with a 3 sec exposure time were collected for each sample. Raman shifts were calibrated with toluene as an internal standard. The data were processed by using CSMA software (Princeton Instruments, Inc. Version 2.4A) on a Gateway 2000 computer, and the resulting ASCII files were processed with Kaleidagraph (Abelbeck Software).

Synthetic methods: General procedures for stoichiometric reactions of 1 or 2 at −77 °C

All reactions were monitored by low-temperature UV–vis spectroscopy. The dewar was equipped with a stir bar and loaded in the drybox with 5.0 mL of a 0.50–1.0 mM solution of the diiron(II) precursor of **1** or **2**. The apparatus was topped with a rubber septum, brought out of the drybox, placed under a positive N_2 pressure, and cooled to −77 °C with a dry ice acetone bath. A spectrum was recorded, and then the sample was subjected to a gentle purge of O_2 at atmospheric pressure for 15 s. After this time the peroxo complex **1** or **2** had formed to completion, as judged by the blue color which developed and the known second order rate constants for the oxygenation reactions. Excess O_2 was removed with a 5 min Ar purge of the solution. Another spectrum was recorded, and then 200 μL of the test reagent solution was added dropwise to a stirred solution of the peroxo complex, taking care not to allow the peroxo solution to warm above −77 °C. For the CO_2 reactions, the gas was bubbled gently through the solution of the peroxo complex over ~30 s. **CAUTION: Owing to the low temperature, this procedure introduces a large excess of CO_2 to the solution, and therefore considerable caution should be taken when venting the solution upon warming so as to not build up a dangerous pressure level**. The resulting mixture was allowed to stir for 15–30 s, by which time a homogenous solution had formed. Additional spectra were recorded, and the reaction was monitored by the decay of the peroxo-to-iron charge transfer band. The quantities of reagents and solvent used for each reaction are listed in Table 1.

General procedures for solvent oxidation studies

Samples were prepared in the immersion dewar described above or in a round bottom flask sealed with a rubber septum. All sample volumes were 5.0 mL. Peroxo complex **1** was generated in the usual manner at −77 °C.[40] It was stable for at least several hours at this temperature, as judged by UV–vis spectroscopy, which afforded identical traces in all the solvents. For thermolysis reactions carried out under argon, the peroxo solution was degassed by carrying out three vacuum/Ar purge cycles and three freeze–pump–thaw cycles with liquid nitrogen, and then backfilling with 1 atm of Ar prior to warming. Warming to room temperature over 5 min was accomplished by removing the reaction vessel from the dry ice/acetone bath. Warming over 2 h was carried out by removing the excess dry ice from the cooling bath while keeping the flask or UV–vis cell in contact with the bath. Solutions incubated at low temperature for longer time periods were placed in a −85 °C refrigerator. After addition of an internal standard, the crude reaction mixtures were examined directly by GC and GC/MS analyses.

Intermolecular kinetic isotope measurements

Peroxo complex samples (1.0 mM) were prepared in equimolar quantities of perdeutero or protio solvents, to a total volume of 5.0 mL. Thermolyses were carried out over 5 min as described above, and the crude reaction mixtures were analyzed by GC/MS.

Results and Discussion

Reactions of peroxide complexes 1 and 2 at −77 °C

The electronic spectra of the 1-alkylimidazole and pyridine complexes **1** and **2** were used to monitor their reactivity toward three classes of substrates: oxygen-atom acceptors, electrophiles/acids, and weak H-atom donors. Such a comparative analysis has been used previously to characterize transition metal peroxo complexes, where the reactivity pattern of the peroxide ligand depends on the Lewis acidity of the metal ion and the mode of peroxo coordination.[44–46] In general, early transition metal ions in high oxidation states render coordinated peroxide ligands electron deficient such that they typically undergo oxygen-atom transfer reactions to acceptors such as phosphines and olefins.[46,47] These reactions become more favored thermodynamically

Table 1. A summary of reagents and solvents used for the stoichiometric reactions

Reagents	Reagent quantity	Peroxo complex	Quantity of diiron(II) precursor (mg, μmol)	Solvent (5.0 mL)
Triphenylphosphine	6.0 mg, 23 μmol	1	5.0, 3.3	THF
2-Cyclohexen-1-one	6.0 mg, 23 μmol	1	6.5, 4.3	THF
Dimethylbenzylamine	10 μL, 66 μmol	1	10, 6.6	Et_2O
2,4-Di-*tert*-butylphenol	1.0 mg, 4.9 μmol	1	7.4, 4.9	THF
2,4-Di-*tert*-butylphenol	1.0 mg, 4.9 μmol	2	7.0, 4.1	CH_2Cl_2
Phenol	0.5 mg, 5.3 μmol	1	6.8, 4.5	THF
Pentafluorophenol	0.7 mg, 3.5 μmol	1	4.8, 3.2	THF
2,4,6-Tri-*tert*-butylphenol	5 μL, 5 μmol	1	6.4, 4.2	Cyclopentane
1-Phenylcyclohexylcarboxylic acid	1.0 mg, 4.7 μmol	1	6.5, 4.3	Toluene
CO_2	Excess	1	7.4, 4.9	Et_2O
CO_2	Excess	2	7.0, 4.1	CH_2Cl_2
Pentamethylferrocene	1.4 mg, 4.4 μmol	1	6.0, 4.0	THF
Cobaltocene	0.8 mg, 4.4 μmol	1	6.0, 4.0	THF

as the substituents bound to the reacting substrate functionality are more electron releasing. By contrast, low-valent, late-metal peroxo adducts usually behave as nucleophiles, undergoing addition reactions to electrophiles such as CO_2, acyl chlorides, or electron-deficient olefins.[46] In addition, these electron rich peroxo adducts will react with acids to afford hydroperoxo complexes or they may react with an additional acid equivalent to liberate H_2O_2. Peroxo complexes may also display radical character and react with weak hydrogen atom donors such as isopropyl C–H[48,49] and phenolic O–H[44,45] bonds. Peroxo O–O bond cleavage may occur prior to hydrogen atom abstraction in these reactions, as has been demonstrated in a related bis(μ-oxo)dicopper system.[50–52] Moreover, the distinction between nucleophilic/basic versus radical peroxo character can be probed with phenols since deprotonation usually leads to phenoxide coordination,[46] whereas hydrogen atom abstraction provides a phenoxyl radical. With appropriate substitution of the aryl ring, such a species can be identified as the 2,2′-biphenol-coupled product.[44,53]

Stoichiometric reactions were conducted by generating peroxo complex **1** or **2** in solution at −77 °C, followed by thorough removal of excess O_2 with Ar purge/dynamic vacuum cycles and then addition of the reagent. Reactions were monitored by UV-vis spectroscopy. These studies are summarized in Scheme 1. No reaction with triphenylphosphine was observed for peroxo adducts **1** or **2**, a result which suggests that they have little or no electrophilic character. Similarly, exposure of either peroxo complex to the weak H-atom donor dimethylbenzylamine afforded no reaction.

Treatment of the 1-butylimidazole peroxo complex **1** with 1.0 equiv of 2,4-di-*tert*-butylphenol resulted in a color change from purple to deep royal blue within 30 s. By contrast, pyridine analogue **2** did not react with the phenol under similar conditions. The optical spectrum of the **1** + phenol reaction product persists for > 2 h at −77 °C, but decays rapidly (< 1 min) upon warming to room temperature (Fig. 1). No 2,2′-biphenol coupled product was detected by GC/MS, as judged by comparison of the product chromatogram to that of pure 2,2′-biphenol, but H_2O_2 was qualitatively identified. These facts, coupled with the metastable nature of the product and the resemblance of its UV–vis spectrum to that of **1**, suggested that a diiron(III) phenoxide–hydroperoxide complex might have been formed through deprotonation of the phenol with the diiron(III)-bound peroxide. The resulting charge transfer band at 620 nm ($\varepsilon = 1400\ M^{-1}\,cm^{-1}$) is considerably red-shifted from those of known hydroperoxo complexes, however, such as $[Fe^{III}(N4Py)(OOH)(MeCN)](ClO_4)_2$($\lambda_{max}$ = 458 mn, $\varepsilon = 1100\ M^{-1}\,cm^{-1}$, where N4Py = N,N-bis(2-pyridylmethyl)-N-bis(2-pyridyl)methylamine)[54] and $[Fe(TPA)(OOH)](ClO_4)]^{2+}$ (λ_{max} = 538 nm, $\varepsilon \sim 1000\ M^{-1}\,cm^{-1}$), where TPA = tris(2-pyridylmethyl)amine).[26] Moreover,

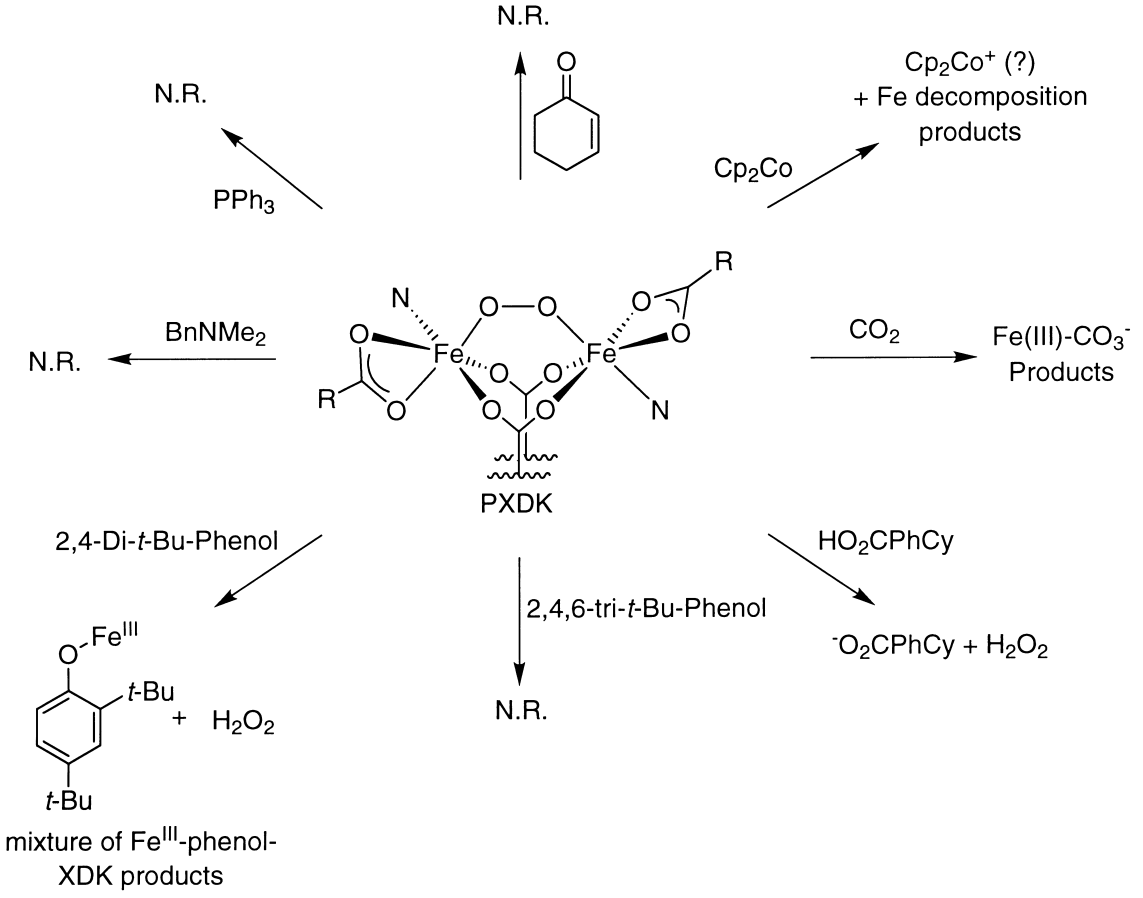

Scheme 1.

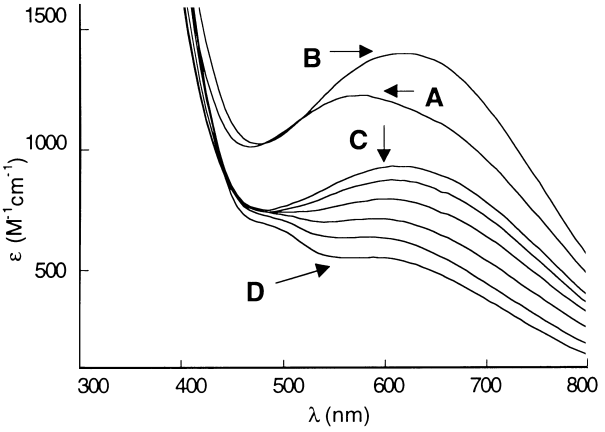

Figure 1. Electronic absorption spectra of **1** in THF at −77 °C (**A**, 0.98 mM), 1.0 equiv of 2,4-di-*tert*-butylphenol added (**B**, λ_{max} = 620 nm, ε = 1400 M^{-1} cm^{-1}), five traces qualitatively tracking the decay of the phenol product upon thermolysis from −77 °C to room temperature (**C**), and the decomposition product at room temperature (**D**).

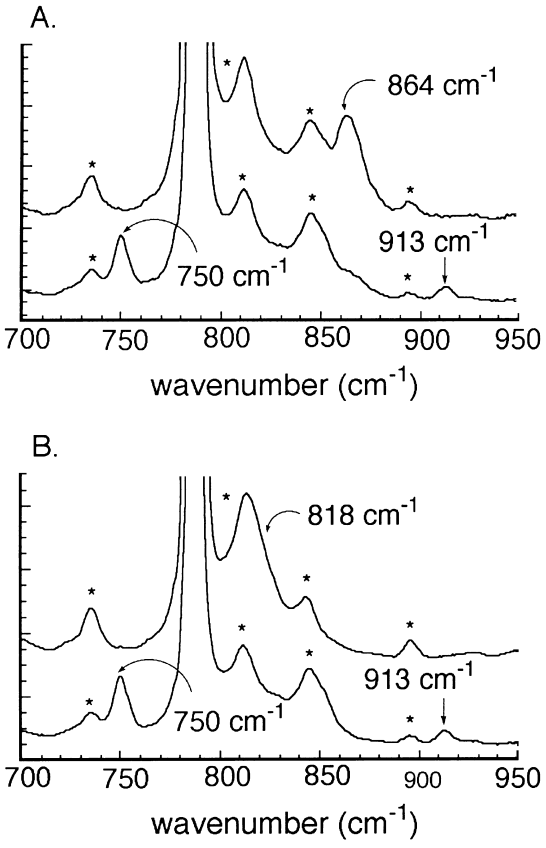

Figure 2. Resonance Raman spectra obtained with 647-nm excitation at −77 °C on fluid toluene solutions of $[Fe_2(^{16}O_2)(PXDK)(O_2CPhCy)_2(Bu\text{-}Im)_2]$ (**A**, top spectrum), **1**-$^{16}O_2$ + 1.1 equiv of 2,4-di-*tert*-butylphenol (**A**, bottom spectrum), $[Fe_2(^{18}O_2)(PXDK)(O_2CPhCy)_2(Bu\text{-}Im)_2]$ (**B**, top spectrum), **1**-$^{18}O_2$ + 1.1 equiv of 2,4-di-*tert*-butylphenol (**B**, bottom spectrum). Peaks marked with an asterisk and those off scale are due to toluene.

reactions with less electron-rich phenols such as the parent compound and pentafluorophenol exhibited UV–vis bands blue-shifted from that obtained for the 2,4-di-*tert*-butylphenol product (C_6H_5OH: λ_{max} = 546 nm, ε = 2100 M^{-1} cm^{-1}; C_6F_5OH: λ_{max} = 460 nm, ε = 3300 M^{-1} cm^{-1}). Both of these observations make it more likely that the product UV–vis feature is due to a phenoxide-to-iron(III) charge transfer.

Resonance Raman studies were conducted to probe further the fate of the peroxide complex **1** upon treatment with 2,4-di-*tert*-butylphenol. Peroxo species were prepared with $^{16}O_2$ or $^{18}O_2$, and each was treated with 1.1 equiv of the phenol. Spectra before and after the reaction are displayed in Figure 2. For the $^{16}O_2$ sample, the ν(^{16}O–^{16}O) band at 864 cm^{-1} disappears almost completely upon addition of the phenol, and two new bands appear at 750 and 913 cm^{-1}. The ν(^{18}O–^{18}O) band also diminishes when phenol is added, as judged by the narrowing and shifting of a peak at ~825 cm^{-1}, which is composed of the peroxo band and one arising from toluene.[40] The same two new peaks observed when phenol was added to the $^{16}O_2$ sample also appear in the $^{18}O_2$ spectrum at identical energies, indicating that neither can be ascribed to a hydroperoxide or peroxide species. These features are therefore assigned to coordinated phenoxide ligand vibrations which are resonance enhanced by a charge transfer band to iron. A new ν(O–O) band may have been obscured by the toluene peaks, but none was observed after performing solvent subtraction procedures.

Irrespective of the identity of the initial metastable products, this set of experiments demonstrate that **1** behaves as a basic, and not a hydrogen atom abstracting, peroxo species. The fact that **2** does not react at all with 2,4-di-*tert*-butylphenol further supports this conclusion. Compared to pyridine, the more basic 1-alkylimidazole groups impart additional electron density to the iron centers in **1**, which is in turn transmitted to the peroxide ligand. Moreover, the difference in the pK_a values for protonated 1-butylimidazole (6.95) and pyridine (5.25) compared to phenol (9.89)[55] makes proton transfer to a dissociated nitrogen instead of the peroxo ligand highly improbable.

Two other proton donors were investigated to probe further the character of the peroxide ligands in **1** and **2**. Treatment of **1** with 1.1 equiv of 2,4,6-tri-*tert*-butylphenol afforded no reaction, as judged by UV–vis spectroscopy. Apparently proton transfer does not occur in this case because the sterically encumbered phenol cannot access the peroxide ligand. Alternatively, the deprotonated phenol may be too hindered to bind to the iron center(s). A carboxylic acid was used to determine whether a hydroperoxo complex could be stabilized by an additional hindered carboxylate ligand and to see whether the less basic pyridine peroxo complex **2** could be protonated with a stronger acid. Treatment of peroxo complex **1** with 1.1 equiv of 1-phenylcyclohexylacetic acid was accompanied by decomposition at −77 °C within 15–30 s (Fig. 3), yielding intractable products upon work up at room temperature. As with all the phenol reactions with **1**, H_2O_2 was detected qualitatively in the crude decomposition mixtures. Peroxo **2** was completely unreactive toward the carboxylic acid, an outcome

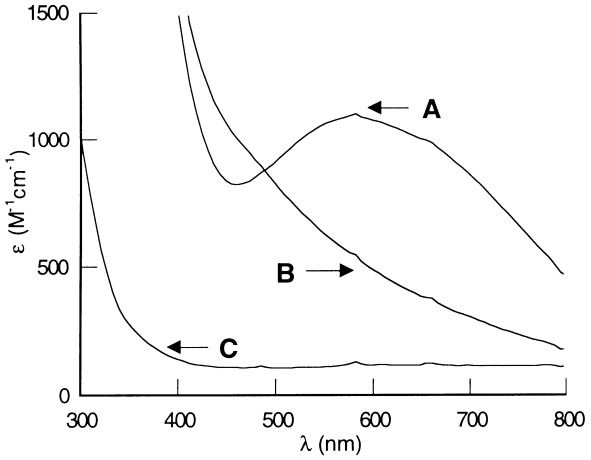

Figure 3. Electronic absorption spectra of **1**-$^{16}O_2$ in toluene at −77 °C (**A**, 0.86 mM), after 1.1 equiv of HO_2CPhCy was added (**B**), and the reduced complex (**1**) prior to addition of $^{16}O_2$ at −77 °C (**C**).

which further illustrates the different electronic properties imparted to the peroxo ligands solely by the choice of N-donor.

Electrophilic reagents were examined to probe the nucleophilicity of the peroxo complexes. Exposure of **1** at −77 °C to a large excess of CO_2 resulted in decay of the peroxide-to-iron charge transfer band within 15 s (Fig. 4). As with other peroxo complexes that react with CO_2,[44,46] this reaction probably generates a peroxycarbonate species which decomposes to an iron(III) carbonate complex(es), although nothing tractable was isolated from the reaction mixture. Consistent with the protonolysis studies, **2** was unreactive toward CO_2 over the course of 2 h as determined by UV–vis spectroscopic monitoring of the reaction. Neither **1** nor **2** was reactive toward 2-cyclohexen-1-one, a less potent electrophile that reacts with some nucleophilic peroxo complexes.[56]

Finally, the behavior of **1** toward reductants was examined to obtain an estimate of its reduction potential. No reaction was observed with ferrocene or pentamethylferrocene, but treatment with cobaltocene induced rapid decay of the peroxo UV–vis band (Fig. 5). The cobaltocenium cationic product could not be identified because intense features in the higher energy visible region dominated the spectrum. Assuming that cobaltocene donates an electron to the peroxo complex in a 1:1 stoichiometry, then the reduction potential of **1** can be estimated to be between those of Cp_2Fe and cobaltocene, −0.59 and −1.33 mV versus Cp_2Fe^+/Cp_2Fe, respectively.[57] This value is consistent with the stability of the diiron(III) peroxo species toward hydrogen atom donors, notwithstanding the issue of proton affinity, since reduction of one of the Fe(III) ions would have to accompany hydrogen atom transfer to the peroxo ligand. Moreover, it provides at least a partial explanation as to why peroxo species **1** deprotonates 2,4-di-*tert*-butylphenol instead of abstracting a hydrogen atom from this reagent.

Thermolysis reactions leading to solvent oxidation

Solutions of peroxo complexes **1** or **2** rapidly decay when warmed above ~−65 °C, changing from purple or midnight blue, respectively, to an orange brown color which is characteristic of μ-oxo diiron(III) complexes. Several mechanisms could account for this decay. The most well documented such reaction in diiron(III) peroxo chemistry is a bimolecular decomposition accompanied by extrusion of 0.5 equiv of O_2 per diiron complex, affording oxo-bridged diiron(III) products.[58,59] Such a process could not entirely account for the decomposition of **1** or **2**, however, because manometric studies indicated either that O_2 was not released during the decay or that, in solvents such as THF and CH_2Cl_2, up to an additional equivalent of dioxygen was consumed.[40] Such a result might be explained a priori by ligand oxidation, but a thorough ^1H NMR, IR, and GC/MS analysis of the organic components revealed no oxidized ligands following acid decomposition and extraction of the resulting products. Instead, solvent oxidation products were identified in the reaction

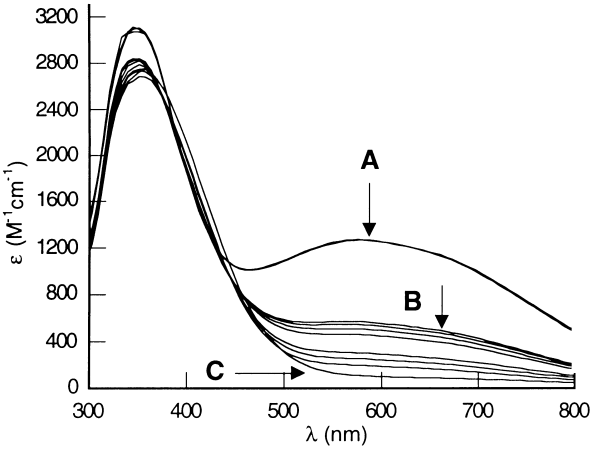

Figure 4. Electronic absorption spectrum of **1** in Et_2O at −77 °C (**A**, 0.98 mM), seven traces qualitatively tracking the decay of the peroxo upon addition of CO_2 at −77 °C (**B**), and the product mixture at −77 °C (**C**).

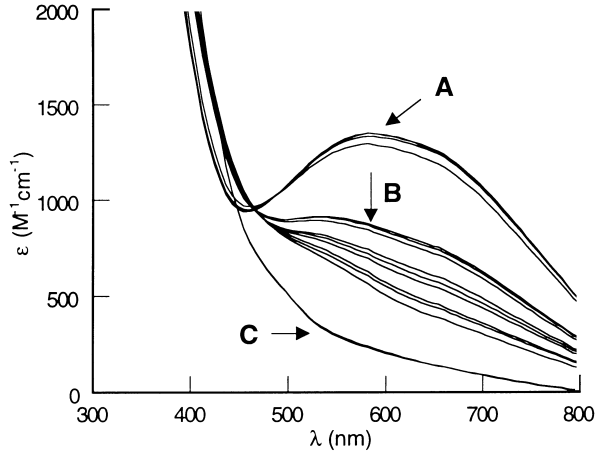

Figure 5. Electronic absorption spectrum of **1** in THF at −77 °C (**A**, 0.79 mM), 11 traces qualitatively tracking the decay of the peroxo upon addition of 1.1 equiv of Cp_2Co (**B**), and the product mixture at −77 °C (**C**).

mixtures for several different solvents. A detailed analysis of those reactions for **1** was undertaken because its butyl and propyl groups render it soluble in a wide variety of hydrocarbons.

Table 2 summarizes the results of this initial survey, which defined the scope of the oxidation process. Substrates with particularly weak C–H bonds,[55] such as THF (92 kcal/mol), cyclohexene (allylic C–H = 85 kcal/mol), and toluene (85 kcal/mol), afforded γ-butyrolactone and 2-hydroxytetrahydrofuran, 2-cyclohexen-1-ol, 2-cyclohexen-1-one, and cyclohexene oxide, and benzaldehyde, respectively, in modest yields based on **1**. 1,2-Dichloroethane, identified qualitatively as a product of peroxo decay in CH_2Cl_2 solutions, was presumably formed by C–Cl bond homolysis. Solvents with high C–H bond strengths, such as isopentane (95 kcal/mol) and pentane (98 kcal/mol), were completely unreactive. Cyclopentane, which has an intermediate C–H bond strength (94.5 kcal/mol), afforded a small amount of product.

Table 2. A survey of solvent oxidation reactions mediated by peroxo **1**

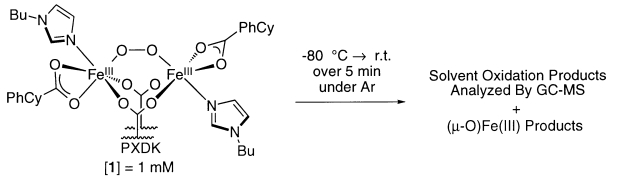

Solvent	Products (% yield based on **1**)
	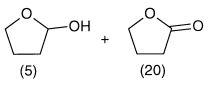 (5) (20)
CH_2Cl_2	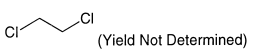 (Yield Not Determined)
	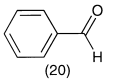 (20)
	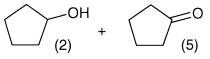 (2) (5)
	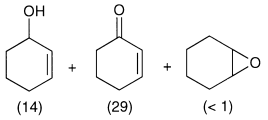 (14) (29) (< 1)
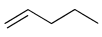	No reaction
	No reaction
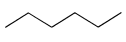	No reaction

A key to understanding this chemistry is provided by the product distribution for each substrate. For cyclohexene, only allylic oxidation products were produced in appreciable quantities. This result contrasts with that for sMMO,[60,61] and early transition metal peroxo[47] or terminal oxo complexes,[62] which all afford the epoxide as the major or exclusive product in reactions with olefins. For oxidations with **1** at saturated C–H bonds, ketones are favored over alcohol products, whereas sMMO affords alcohols exclusively.[60,61]

To investigate the mechanism in more detail, we chose to focus on cyclopentane oxidation. This solvent is readily purified and not susceptible to autoxidation in air for months at room temperature. Cyclohexene and THF, on the other hand, autoxidize after ~12 h in air in the absence of radical inhibitors, judging by GC/MS. From a practical standpoint its higher C–H bond strength makes cyclopentane a more attractive target.

Table 3 lists a series of conditions designed to probe the oxidation mechanism of cyclopentane. The results for entries 1–3 reveal that yields of ketone and alcohol are unaffected by the warming rate, reaction atmosphere, or peroxo concentration; in each case the same small quantities of ketone and alcohol formed in a 2.5:1 ratio. When decomposed reaction mixtures were allowed to stand in air for extended periods of time (entries 6–8), however, a slow but steady production of additional product resulted, as determined by analyzing aliquots of the reaction mixture by GC/MS on a daily basis. After three weeks the total yield of oxidized products based on the original amount of **1** was 250%, but the ketone:alcohol ratio remained invariant over this time period. The latter observation suggests that the entire oxidation process proceeds through a common mechanism, from the initial warming of the peroxo solution through prolonged incubation in air at room temperature. An aliquot of the long-term reaction was removed after 1 day (entry 8) and treated with a 50-fold excess of 2,4,6-*tert*-butylphenol, which completely quenched product formation. Moreover, when solutions of **1** were warmed in the presence of 1.0 equiv of this phenol, with which it does not react at −77 °C (vide supra), no oxidized products were observed either immediately after the reaction or upon standing in air for several days.

An intermolecular kinetic isotope effect (KIE) was not measured for cyclopentane oxidation because the perdeutero isotopomer is prohibitively expensive. Instead, we carried out measurements using THF and toluene as solvents, which afforded k_H/k_D values of 6.2 and 7.8, respectively. These values may be compared to the intramolecular KIE values of 2–3 for Gif cyclohexane and adamantane oxidations,[63] and 1.0 for sMMO.[24]

The ability of phenol to quench product formation indicates that a free radical, non-metal based autoxidation mechanism is most likely occurring for this system. An example of such a mechanism is illustrated by eqs (2)–(5) for oxidation at a secondary carbon atom.[46] This well known hydrocarbon oxidation process is initiated by

Table 3. Cyclopentane oxidation reactions carried out with peroxo **1** under a set of experimental conditions designed to probe the mechanism

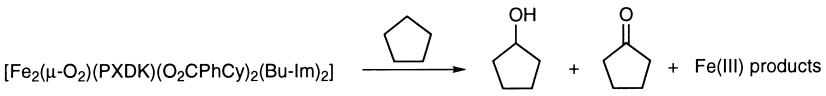

Entry	atm	Temp. (°C)/Heating rate	Concn (mM)	Additives (equiv)	Yield (%)	
					-one	-ol
1	Ar or O_2	−77→rt over 5 min	1.2	None	5	2
2		−77→rt over 2 h	1.2		5	2
3		−85 for 3 days	1.2		5	2
4		−77→rt over 5 min	0.12		5	2
5		−77→rt over 5 min	11.2		5	2
6	Ar or O_2, then air	−77→rt over 5 min then rt, 24 h	1.2		10	4
7		−77→rt over 5 min then rt, 3 weeks			170	80
8		−77→rt over 5 min then rt, 3 weeks		2,4,6-*t*-Bu-phenol (10) after 24 h	10	4
9	Ar or O_2	−77→rt over 5 min		2,4,6-*t*-Bu-phenol (10)	0	0
10		−77→rt over 5 min		PPh_3 (1.0)	5	2
11		−77→rt over 5 min		HO_2CPhCy (10) or H_2O (10)	5	2

$$\textit{Initiation}\ \ In\cdot + R_2CH_2 \longrightarrow InH + R_2CH\cdot \qquad (2)$$

$$\textit{Propagation}\ \ R_2CH\cdot + O_2 \longrightarrow R_2CHOO\cdot \qquad (3)$$

$$R_2CHOO\cdot + R_2CH_2 \longrightarrow R_2CH\cdot + R_2CHOOH \qquad (4)$$

$$\textit{Termination}\ \ 2R_2CHOO\cdot \longrightarrow R_2CO_4CR_2 \longrightarrow R_2CHOH + R(CO)R + O_2 \qquad (5)$$

hydrogen atom abstraction to generate an alkyl radical, which is trapped with dioxygen. The resulting alkyl peroxy radical then reacts with another equivalent of substrate, and the chain is propagated. Chain termination occurs when two alkyl peroxy radicals combine, and the resulting species rearranges to afford dioxygen, ketone, and alcohol. Decomposition of the resulting alkyl hydroperoxide to ketone and alcohol can be catalysed by iron salts via a Haber–Weiss cycle (eqs (6) and (7)).[62,64] The resulting alkoxy radical reacts with substrate to yield alcohol (eq (8)), and the alkyl peroxy radical can decompose as indicated in eq (5).

$$Fe(II) + R_2CHOOH \longrightarrow R_2CHO\cdot + Fe^{III}(OH) \qquad (6)$$

$$Fe^{III}(OH) + R_2CHOOH \longrightarrow R_2CHOO\cdot + Fe^{II} + H_2O \qquad (7)$$

$$R_2CHO\cdot + R_2CH_2 \longrightarrow R_2CH\cdot + ROH \qquad (8)$$

The reaction mixtures were analyzed by ^1H NMR and GC/MS to determine whether a significant concentration of cyclopentylhydroperoxide builds up over the course of the extended reactions. No ^1H NMR resonances or GC/MS peaks attributable to this species were identified upon comparing the data to that obtained for a pure sample prepared independently. A peroxo sample was also warmed in the presence of 10 equiv of PPh_3 to trap any cyclopentylhydroperoxide that might have formed, a reaction which would afford triphenylphosphine oxide and alcohol. This procedure neither changed the overall yield nor altered the ketone:alcohol ratio, suggesting that if the hydroperoxide is formed it decomposes exceedingly rapidly.

Perhaps the most interesting issue for this system is the role of **1** in the autoxidation chemistry. For reactions conducted under Ar, the peroxo is presumably the source of free O_2, some of which could be released upon warming. In addition, it is highly probable that a metal-bound oxygen species is involved in the initiation step. One possibility would be direct hydrogen atom abstraction by the diiron(III) peroxide, affording a Fe(II)Fe(III) hydroperoxo complex and an alkyl radical (eq (9)). The former could then eliminate a hydroxyl radical and a (μ-oxo)diiron(III) product (eq (10)).

$$[Fe^{III}_2(\mu - O_2)(XDK)(O_2CPhCy)_2(Bu - Im)_2] + C_5H_{10} \longrightarrow [Fe^{II}Fe^{III}(OH)(XDK)(O_2CPhCy)_2(Bu - Im)_2] + C_5H_9\cdot \qquad (9)$$

$$[Fe^{II}Fe^{III}(OH)(XDK)(O_2CPhCy)_2(Bu - Im)_2] \longrightarrow [Fe^{III}_2(\mu - O)(XDK)(O_2CPhCy)_2(Bu - Im)_2] + OH\cdot \qquad (10)$$

This particular sequence of events is unlikely, however, since **1** displays no propensity to abstract a hydrogen atom from even weak H-atom donors such as phenol (O–H bond strength = 88 kcal/mol).[55] Alternatively, the peroxo complex may convert to a new intermediate upon warming that is capable of performing the hydrogen atom abstraction reaction. Perhaps a dioxodiiron(IV) species forms having the same formal metal oxidation states as sMMO-Q but exhibiting a much different pattern of reactivity (eq (11)). More likely perhaps is a bimolecular decay, whereby some of the

peroxo complex releases O_2 upon warming, and the resulting reducing equivalents are then used to activate diiron(III) peroxide to effect Fenton chemistry, perhaps with trace water serving as a proton source to generate a hydroxyl radical (eq (12)).

$$[Fe_2^{III}(\mu-O_2)(XDK)(O_2CPhCy)_2(Bu-Im)_2] \xrightarrow[\text{homolysis}\,\Delta]{O-O\ \text{bond}} [Fe_2^{IV}(O)_2(XDK)(O_2CPhCy)_2(Bu-Im)_2] \xrightarrow{C_5H_9} C_5H_9\cdot \quad (11)$$

$$\left[Fe_2^{III}(\mu-O_2)(XDK)(O_2CPhCy)_2(Bu-Im)_2\right] \overset{\Delta}{\rightleftharpoons} \left[Fe_2^{II}(XDK)(O_2CPhCy)_2(Bu-Im)_2\right] \xrightarrow[\mathbf{1},H^+]{} OH\cdot + \text{Fe(III) Products} \quad (12)$$

An important conclusion to be drawn from these cyclopentane oxidation studies is that, despite having generated a stoichiometrically accurate model of the H_{peroxo} intermediate, we have not accessed the manifold of reactivity used by the diiron centers in sMMO in terms of substrate scope, product selectivity, or the oxidation mechanism. A similar diiron(III) peroxo adduct has been suggested as a key intermediate in iron(III)-catalyzed hydrocarbon oxidations with H_2O_2,[27] but these systems also lack sMMO selectivity and radical pathways have been implicated.[30,37] Conversely, studies of the enzyme with radical clock substrate probes and chiral ethane have provided evidence against a discrete radical intermediate.[24,25] Hence, for a functional model system to duplicate the chemistry of sMMO, metal-based oxidants which abstract hydrogen from a substrate without concomitantly forming a carbon–oxygen bond must be avoided. Not only might such a reaction lead to undesired radical chain autoxidation chemistry, but it would also imply that the model has not matched the composition and structure of the key enzymatic oxidant.

Recent X-ray studies of resting state MMOH[65] and EXAFS studies on intermediate Q[18] provide some insight into why the diiron XDK system may not be able to mimic the enzymatic chemistry and suggest new design strategies for improved functional models. In the resting enzyme, only one carboxylate ligand bridges the diiron center. The short Fe···Fe distance of 2.5 Å observed for intermediate Q cannot be accommodated by a *syn,syn*-bidentate bis(carboxylate)bridged core, and it is unlikely that the rigid XDK ligand system possesses the flexibility to undergo the carboxylate shift[66] required to convert peroxo adducts **1** or **2** into Q-like diiron(IV) complexes. Alternatively, ligands which provide a single *syn,syn*-bidentate carboxylate bridge while maintaining a rigid dinucleating framework may provide ideal balance for converting a peroxo adduct into a Q-like species. Efforts to prepare such complexes in this laboratory have recently provided encouraging preliminary results.[67]

Conclusions

The reactivity properties of diiron(III) peroxo complexes **1** and **2** have been fully elucidated. These adducts behave as nucleophilic/basic peroxides, exhibiting no tendency to serve as oxygen atom donors, even for potent acceptors such as triphenylphosphine. The 1-butylimidazole ligands in **1** enhance the nucleophilicity/basicity of the peroxo ligand compared to the pyridine analogue probably because imidazole is a better σ-donor. This greater electron density at the iron centers would be transmitted to the peroxo ligand. Thermolysis of the peroxo adducts in a variety of media results in solvent oxidation, providing ketone and alcohol products in modest yields based on the complex. A detailed analysis of cyclopentane oxidation provided evidence for a radical chain autoxidation mechanism, a reaction manifold which does not mimic the hydrocarbon oxidation chemistry of sMMO. Future efforts are aimed at preparing diiron(III) peroxo complexes having carboxylate-bridged structures that facilitate conversion to a Q-type unit to allow access to the enzymatic hydroxylation pathway.

Acknowledgements

This work was supported by grants from the National Science Foundation and AKZO Corp. We thank A. M. Valentine, D. P. Steinhuebel, and J. D. Du Bois for many helpful discussions.

References

1. Karasevich, E. I.; Kulikova, V. S.; Shilov, A. E.; Shteinman, A. A. *Russ. Chem. Rev.* **1998**, *67*, 335.
2. Shilov, A. E. *Metal Complexes in Biomimetic Chemical Reactions*; CRC Press: Boca Raton, FL, 1997.
3. Shilov, A. E.; Shul'pin, G. B. *Chem. Rev.* **1997**, *97*, 2879.
4. Arndsten, B. A.; Bergman, R. G.; Mobley, T. A.; Peterson, T. H. *Acc. Chem. Res.* **1995**, *28*, 154.
5. Sommer, J.; Bukala, J. *Acc. Chem. Res.* **1993**, *26*, 370.
6. Hill, C. L. Activation and Functionalization of Alkanes; Wiley & Sons: New York, 1989.
7. Periana, R. A.; Taube, D. J.; Gamble, S.; Taube, H.; Satoh, T.; Fujii, H. *Science* **1998**, *280*, 560.
8. Lin, M.; Hogan, T.; Sen, A. *J. Am. Chem. Soc.* **1997**, *119*, 6048.
9. Wallar, B. J.; Lipscomb, J. D. *Chem. Rev.* **1996**, *96*, 2625.
10. Liu, K. E.; Lippard, S. J. In *Advances in Inorganic Chemistry*; Sykes, A. G., Ed.; Academic Press: San Diego, CA, 1995; pp 263–289.
11. Feig, A. L.; Lippard, S. J. *Chem. Rev.* **1994**, *94*, 759.
12. Solomon, E. I.; Sundaram, U. M.; Machonkin, T. E. *Chem. Rev.* **1996**, *96*, 2563.
13. Semrau, J. D.; Zolandz, D.; Lidstrom, M. E.; Chan, S. I. *J. Inorg. Biochem.* **1995**, *58*, 235.
14. Valentine, A. M.; Lippard, S. J. *J. Chem. Soc., Dalton Trans.* **1997**, 3925.
15. Edmondson, D. E.; Huynh, B. H. *Inorg. Chim. Acta* **1996**, *252*, 399.
16. Liu, K. E.; Valentine, A. M.; Wang, D.; Huynh, B. H.; Edmondson, D. E.; Salifoglou, A.; Lippard, S. J. *J. Am. Chem. Soc.* **1995**, *117*, 10174.
17. Valentine, A. M.; Tavares, P.; Pereira, A. S.; Davydov, R.; Krebs, C.; Hoffman, B. M.; Edmondson, D. E.; Huynh, B. H.; Lippard, S. J. *J. Am. Chem. Soc.* **1998**, *120*, 2190.

18. Shu, L.; Nesheim, J. C.; Kauffmann, K.; Munck, E.; Lipscomb, J. D., Que, L., Jr. *Science* **1997**, *275*, 515.
19. Sturgeon, B. E.; Burdi, D.; Chen, S.; Huynh, B. H.; Edmondson, D. E.; Stubbe, J.; Hoffman, B. M. *J. Am. Chem. Soc*. **1996**, *118*, 7551.
20. Willems, J.-P.; Lee, H.-I.; Burdi, D.; Doan, P. E.; Stubbe J.; Hoffman, B. M. *J. Am. Chem. Soc*. **1997**, *119*, 9816.
21. Burdi, D.; Riggs-Gelasco, P.; Tong, W.; Willems, J.-P.; Lee, H.-I.; Doan, P. E.; Sturgeon, B.; Shu, L.; Chen, S.; Que, L., Jr.; Hoffmann, B. M.; Stubbe, J.; Edmondson, D. E.; Huynh, B. H. *Steenbock Symposium Proceedings: Biosynthesis and Function of Metal Clusters for Enzymes* **1997**, *25*, 85.
22. Bollinger, J. M., Jr.; Krebs, C.; Vicol, A.; Chen, S.; Ley, B. A.; Edmondson, D. E.; Huynh, B. H. *J. Am. Chem. Soc*. **1998**, *120*, 1094.
23. Moënne-Loccoz, P.; Baldwin, J.; Ley, B. A.; Loehr, T. M.; Bollinger, J. M., Jr. *Biochemistry* **1998**, *37*, 14659.
24. Liu, K. E.; Johnson, C. C.; Newcomb, M.; Lippard, S. J. *J. Am. Chem. Soc*. **1993**, *115*, 939.
25. Valentine, A. M.; Wilkinson, B.; Liu, K. E.; Komar-Panicucci, S.; Priestley, N. D.; Williams, P. G.; Morimoto, H.; Floss, H. G.; Lippard, S. J. *J. Am. Chem. Soc*. **1997**, *119*, 1818.
26. Kim, C.; Chen, K.; Kim, J.; Que, L., Jr. *J. Am. Chem. Soc*. **1997**, *119*, 5964.
27. Barton, D. H. R.; Hu, B.; Taylor, D. K.; Rojas-Wahl, R. U. *J. Chem. Soc. Perkin Trans. 2* **1996**, 1031.
28. Barton, D. H. R.; Doller, D. *Acc. Chem. Res*. **1992**, *25*, 504–512.
29. Ménage, S.; Vincent, J. M.; Lambeaux, C; Fontecave, M. *J. Chem. Soc. Dalton Trans*. **1994**, 2081.
30. Fish, R. H.; Konings, M. S.; Oberhausen, K. J.; Fong, R. H.; Yu, W. M.; Christou, G.; Vincent, J. B.; Coggin, D. K.; Buchanan, R. M. *Inorg. Chem*. **1991**, *30*, 3002.
31. Kim, J.; Harrison, R. G.; Kim, C.; Que, L., Jr. *J. Am. Chem. Soc*. **1996**, *118*, 4373.
32. Ménage, S.; Vincent, J.-M.; Lambeaux, C.; Fontecave, M. *J. Mol. Cat. A, Chem*. **1996**, *113*, 61.
33. Rabion, A.; Chen, S.; Wang, J.; Buchanan, R. M.; Seris, J.-L.; Fish, R. H. *J. Am. Chem. Soc*. **1995**, *117*, 12356.
34. MacFaul, P. A.; Arends, I. W. C. E.; Ingold, K. U.; Wayner, D. D. M. *J. Chem. Soc. Perkin Trans. 2* **1997**, 135.
35. MacFaul, P. A.; Ingold, K. U.; Wayner, D. D. M.; Que, L., Jr. *J. Am. Chem. Soc*. **1997**, *119*, 10594.
36. Minisci, F.; Fontana, F.; Araneo, S.; Recupero, F.; Zhao, L. *Synlett* **1996**, *119*.
37. Newcomb, M.; Simakov, P. A.; Park, S.-U. *Tetrahedron Lett*. **1996**, **37**, 819.
38. Snelgrove, D. W.; MacFaul, P. A.; Ingold, K. U.; Wayner, D. D. M. *Tetrahedron Lett*. **1996**, *37*, 823.
39. Perkins, M. J. *Chem. Soc. Rev*. **1996**, 229.
40. LeCloux, D. D.; Barrios, A. M.; Mizoguchi, T. J.; Lippard, S. J. *J. Am. Chem. Soc*. **1998**, *120*, 9001.
41. van der Linden, A.; Schaverien, C. J.; Meijboom, N.; Ganter, C; Orpen, A. G. *J. Am. Chem. Soc*. **1995**, *117*, 3008.
42. Walling, C.; Buckler, S. A. *J. Am. Chem. Soc*. **1955**, *77*, 6032.
43. Bates, H. A.; Farina, J. *J. Org. Chem*. **1985**, *50*, 3843.
44. Paul, P. P.; Tyeklár, Z.; Jacobsen, R. R.; Karlin, K. D. *J. Am. Chem. Soc*. **1991**, *113*, 5322.
45. Tyeklár, Z.; Karlin, K. D. In *Bioinorganic Chemistry of Copper*; Karlin, K. D., Tyeklár, Z., Eds.; New York: Chapman and Hall, 1993; pp 277–291.
46. Sheldon, R. A.; Kochi, J. K. *Metal-Catalyzed Oxidations of Organic Compounds*; New York: Academic, 1981.
47. Conte, V.; Di-Furia, F.; Moro, S. *J. Phys. Org. Chem*. **1996**, *9*, 329.
48. Reinaud, O. M.; Theopold, K. H. *J. Am. Chem. Soc*. **1994**, *116*, 6979.
49. Hikichi, S.; Komatsuzaki, H.; Kitajima, N.; Akita, M.; Mukai, M.; Kitagawa, T.; Moro-oka, Y. *Inorg. Chem*. **1997**, *36*, 266.
50. Tolman, W. B. *Acc. Chem. Res*. **1997**, *30*, 227.
51. Mahapatra, S.; Halfen, J. A.; Wilkinson, E. C.; Pan, G.; Wang, X.; Young, V. G., Jr.; Cramer, C. J.; Que, L., Jr.; Tolman, W. B. *J. Am. Chem. Soc*. **1996**, *118*, 11555.
52. Mahapatra, S.; Halfen, J. A.; Tolman, W. B. *J. Am. Chem. Soc*. **1996**, *118*, 11575.
53. Kim, C.; Dong, Y.; Que, L., Jr. *J. Am. Chem. Soc*. **1997**, *119*, 3635.
54. Lubben, M.; Meetsma, A.; Wilkinson, E. C.; Feringa, B.; Que, L., Jr. *Angew. Chem., Int. Ed. Engl*. **1995**, *34*, 1512.
55. Lide, D. R. *Handbook of Chemistry and Physics*, 74th Edition; CRC: Boca Raton, 1993.
56. Selke, M.; Sisemore, M. F.; Ho, R. Y. N.; Wertz, D. L.; Valentine, J. S. *J. Mol. Cat. A, Chem*. **1997**, *117*, 71.
57. Connelly, N. G.; Geiger, W. E. *Chem. Rev*. **1996**, *96*, 877.
58. Feig, A. L.; Becker, M.; Schindler, S.; van Eldik, R.; Lippard, S. J. *Inorg. Chem*. **1996**, *35*, 2590.
59. Feig, A. L.; Masschelein, A.; Bakac, A.; Lippard, S. J. *J. Am. Chem. Soc*. **1997**, *119*, 334.
60. Green, J.; Dalton, H. *J. Biol. Chem*. **1989**, *264*, 17698.
61. Colby, J.; Stirling, D. I.; Dalton, H. *Biochem. J*. **1977**, *165*, 395.
62. Sheldon, R. A.; Kochi, J. K. *Advan. Catal*. **1976**, *25*, 272.
63. Singh, B.; Long, J. R.; deBiani, F. F.; Gatteschi, D.; Stavropoulos, P. *J. Am. Chem. Soc*. **1997**, *119*, 7030.
64. Walling, C. *Acc. Chem. Res*. **1975**, *8*, 125.
65. Rosenzweig, A. C.; Brandstetter, H.; Whittington, D. A.; Nordlund, P.; Lippard. S. J.; Frederick, C. A. *Proteins* **1997**, *29*, 141.
66. Rardin, R. L.; Tolman, W. B.; Lippard, S. J. *New J. Chem*. **1991**, *15*, 417.
67. Lee, D.; Lippard, S. *J. Am. Chem. Soc*. **1998**, *120*, 12153.